Contents lists available at ScienceDirect

Arabian Journal of Chemistry

journal homepage: www.ksu.edu.sa

A novel pyrrolidine-2,5-dione derivative induced G2/M phase arrest and apoptosis of hepatocellular carcinoma HepG2 cells through inhibiting tubulin polymerization

Yingying Tian [a], Ailin Yang [a], Huiming Huang [a], Jinxin Xie [a], Longyan Wang [a], Dongxiao Liu [a], Xuejiao Wei [a], Peng Tan [a], Pengfei Tu [a], Dongjun Fu [b,*], Zhongdong Hu [b,*]

[a] School of Chinese Materia Medica, Beijing University of Chinese Medicine, Beijing 100029, China
[b] Beijing Research Institute of Chinese Medicine, Beijing University of Chinese Medicine, Beijing 100029, China

ARTICLE INFO

Keywords:
Pyrrolidine-2,5-dione derivative
Hepatocellular carcinoma
Proliferation
G2/M phase arrest
Apoptosis
Tubulin polymerization

ABSTRACT

Hepatocellular carcinoma (HCC) is a major global cause of carcinoma-related fatality. The inhibition of tubulin polymerization holds significant potential in the development of cancer drugs. In our study, we synthesized a novel pyrrolidine-2,5-dione derivative (compound **8**) that exhibited potent anti-HCC activity (IC_{50} value of 2.082 μM) against human HCC HepG2 cells. Moreover, compound **8** significantly suppressed the HepG2 cell multiplication, and triggered G2/M phase arrest of HepG2 cells and their apoptosis. Further mechanistic investigations revealed that compound **8** suppressed tubulin polymerization by directly binding to the colchicine binding site of β-tubulin. Additionally, compound **8** significantly inhibited tumor growth with low toxicity in nude HepG2 tumor-bearing mice, achieving an approximate inhibition rate of 45.73 %. Therefore, compound **8** represents a promising pharmaceutical candidate for HCC management.

1. Introduction

Apart from being a primary contributor to mortality, cancer presents a significant challenge to extending life expectancy worldwide. Hepatocellular carcinoma (HCC) stands out as one of the most prevalent cancers globally, posing a substantial healthcare burden. Primary hepatic cancer ranks as the sixth most frequently diagnosed cancer and the third leading cause of carcinoma-related deaths worldwide (Sung et al., 2021). Due to late-stage diagnoses, the 5-year survival rate for HCC is less than 5 % among patients with unresectable conditions (Sun and Sarna, 2008). This underscores the need for innovative and resource efficient solutions, as transplantation is often not feasible. Given these circumstances, it becomes imperative to identify novel anticancer agents to enhance treatment response and survival in HCC patients. Microtubules as chief cytoskeletal components, play crucial roles in various cellular processes, including intracellular trafficking, structural support, DNA segregation (Goodson and Jonasson, 2018), spindle formation, apoptosis, and intracellular transportation (Guggilapu et al., 2017). Consequently, microtubules have long been considered a promising target for the development of anticancer agents (Ho et al., 2019). Colchicine-binding site inhibitors are particularly advantageous due to their substantial bioavailability. In the past decade, numerous tubulin polymerization inhibitors have been discovered as potent anticancer agents (Ghawanmeh et al., 2018). Currently, inhibitors such as AVE8062, BNC-105p, CA-4P, and CKD-516 are undergoing clinical trials for anti-carcinoma (Li et al., 2018).

In recent years, pyrrolidine-2,5-dione has emerged as a promising scaffold with potent antitumor activity for the development of anticancer agents in medicinal chemistry. As illustrated in Fig. 1, pyrrolidine-2,5-dione derivative **1** exhibited excellent antiproliferative activity (IC_{50} = 0.78 μM) against MCF7 cells by inhibiting the anti-apoptotic protein Bcl-2 (Tilekar et al., 2020). Pyrrolidine-2,5-dione derivative **2** displayed high cytotoxicity against human breast adenocarcinoma cell lines by inducing ROS production for a potent anticancer effect (Han et al., 2016). Pyrrolidine-2,5-dione derivative **3** demonstrated antiproliferative effects (IC_{50} = 1.58 μM) against cervical carcinoma HeLa cells (Milosevic et al., 2017). Pyrrolidine-2,5-dione derivative **4** exhibited anti-proliferative activity against non-small cell lung cancer, leukemia, and renal carcinoma cells (Luzina and Popov, 2014).

* Corresponding authors at: No. 11 North 3rd Ring East Road, Chaoyang District, Beijing 100029, PR China.
E-mail addresses: fudongjun@bucm.edu.cn (D. Fu), zdhu@bucm.edu.cn (Z. Hu).

https://doi.org/10.1016/j.arabjc.2023.105550
Received 28 September 2023; Accepted 11 December 2023
Available online 14 December 2023

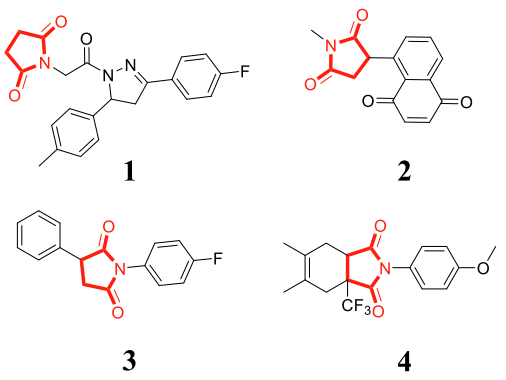

Fig. 1. Pyrrolidine-2,5-dione derivatives with antiproliferative activity.

Building on our prior research (Fu et al., 2018), we identified the tertiary amide moiety as a promising scaffold for designing tubulin polymerization inhibitors. Consequently, we designed and synthesized a novel pyrrolidine-2,5-dione derivative (compound **8**) containing a tertiary amide moiety. Our findings indicate that compound **8** significantly suppressed HepG2 cell proliferation and induced G2/M phase arrest in HepG2 cells. Furthermore, compound **8** upregulated apoptosis in HepG2 cells. Through immunofluorescence, EBI assays, and molecular docking, we demonstrated that compound **8** suppressed tubulin polymerization by directly binding to the colchicine binding site of β-tubulin. Importantly, compound **8** exhibited potent efficacy in combating hepatoma *in vivo*. Thus, compound **8** represents a promising drug candidate for managing HCC.

2. Materials and methods

2.1. Reagents, antibodies, and drugs

DMEM (10–013-CV), FBS (35–010-CV), PBS (21–040-CV), 0.25 % trypsin-EDTA (25–053-CI), and penicillin–streptomycin mixture buffer (30–002-CI) were supplied by Corning Life Sciences (NY, USA). Assay kits for cell cycle (C1052) and apoptosis (C1062L) were products of Beyotime Biotechnology (Shanghai, China). Hoechst 33258 (B2883) and Cell Counting Kit-8 (CCK-8, BN15201) were supplied by Biorigin (Beijing, China). DMSO (purity = 99 %, V900090) and enhanced chemiluminescence (ECL, RPN2232) were separately procured from Sigma (MO, USA) and GE Healthcare (USA). $CDCl_3$ was purchased from InnoChem, China. The β-Actin (sc-47778) antibody was obtained from Santa Cruz Biotechnology (USA). PARP (9532 T), Caspase-7 (9494S), Caspase-9 (9504 T), and cleaved Caspase-8 (8592 T) were products of Cell Signaling Technology (MA, USA). β-Tubulin (BN20622) and DAPI (BN20295) were purchased from Biorigin (Beijing, China). EBI (HY-34477) and colchicine (HY-16569) were obtained from MedChemExpress Company (NJ, USA). Ki67 rabbit monoclonal antibody (AF1738) and TUNEL (C1098) were products of Beyotime Biotechnology (Shanghai, China).

2.2. Cell culture

The human hepatoma cell line HepG2 was obtained from the American Type Culture Collection (Manassas, VA). The cells were cultured in DMEM containing 10 % FBS and 1 % penicillin/streptomycin at 37 °C and 5 % CO2.

2.3. General procedure for the synthesis of compound 6

A 15-mL *N*,*N*-dimethylformamide solution containing 1-(chloromethyl)-4-methoxybenzene **5** (12 mmol) and pyridine (10 mmol) was reacted with 3,4,5-trimethoxyaniline (10 mmol) at 60 °C. After 9 h of agitation, water and dichloromethane were added to dilute the reaction mixture. The organic layer was washed with water and dried with anhydrous magnesium sulfate. The system was then concentrated to yield crude product **6** without purification.

2.4. General procedure for the synthesis of compound 7

Crude product **6** (5 mmol) was added to a 10 mL acetone solution containing chloroacetyl chloride (7 mmol) and potassium carbonate (3.5 mmol) at ambient temperature. After 5 h of agitation, the mixture was filtered, and the system was concentrated to provide crude product **7** without purification. Compounds **6** and **7** were previously reported by (Fu et al., 2018).

2.5. General procedure for the synthesis of compound 8

A solution of crude product **7** (2 mmol) was mixed with potassium hydroxide (2 mmol) and pyrrolidine-2,5-dione (2.5 mmol) in acetonitrile (8 mL). After 8 h of reflux agitation, the system was washed with brine and water, dried with anhydrous magnesium sulfate, filtered and concentrated. The residue was purified by column chromatography (petroleum:ethyl acetate = 9:1) to obtain the target compound **8**. The NMR and MS data supporting the structure of compound **8** are listed in the Supporting Information.

2.5.1. 2-(2,5-Dioxopyrrolidin-1-yl)-N-(4-methoxybenzyl)-N-(3,4,5-trimethoxyphenyl) acetamide (compound 8)

Yield: 47.2 %, white solid, m.p: 164–166 °C. ^{1}H NMR (400 MHz, $CDCl_3$) δ 7.04 (d, J = 8.6 Hz, 2H), 6.74 (d, J = 8.6 Hz, 2H), 6.19 (s, 2H), 4.69 (s, 2H), 3.98 (s, 2H), 3.77 (s, 3H), 3.71 (s, 3H), 3.67 (s, 6H), 2.72 (s, 4H). ^{13}C NMR (100 MHz, $CDCl_3$) δ 175.75, 164.03, 158.14, 152.73, 137.06, 134.88, 129.48, 128.02, 112.76, 104.74, 59.93, 55.23, 54.27, 51.90, 39.29, 27.28. HRMS (ESI): $[M + H]^+$ calcd. for $C_{23}H_{27}N_2O_7$: 443.1813, found: 443.1787.

2.6. MTT assay

After preparing HepG2 cells as single-cell suspensions, they were adjusted to a density of 3.5 × 10^4 cells/mL and plated onto a 96-well microplate, with 100 μL per well. Compound **8** was administered at various doses (0, 0.5, 1, 2, 4, and 8 μM). At 12, 24, and 48 h after drug treatment, MTT (10 μL) was added to each well, followed by a 3-hour incubation of the microplate at 37 °C under light-shielded conditions. Then, the MTT solution was discarded, and each well was treated with DMSO (150 μL). A microplate reader (PerkinElmer EnSpire, USA) was used to measure the 490-nm absorbance (Chen et al., 2020).

2.7. Flow cytometry for apoptosis analysis

HepG2 cells (4 × 10^5 cells/well) were seeded onto a 6-well microplate at an appropriate density and allowed to adhere. Different concentrations of compound **8** were added to subject the cells to an additional 48-h incubation. HepG2 cells were then transferred to an EP tube and centrifuged for 5 min at 1000 rcf and 4 °C. The cells were resuspended in PBS solution and centrifuged again under the same conditions for 5 min. After discarding the supernatant, each sample tube was treated with 1 × binding buffer (200 μL), Annexin V-FITC (2 μL), and propidium iodide (PI, 2 μL). The mixture was gently mixed and incubated for 15 min at room temperature in the absence of light, followed by flow cytometric analysis (BD FACSCantoII, USA) of the cell apoptotic rate using FlowJo software (Ouyang et al., 2023).

2.8. Flow cytometry for cell cycle analysis

HepG2 cells (4 × 10^5 cells/well) were plated onto a 6-well microplate and allowed to attach. After 12 h of cell starvation, compound **8**

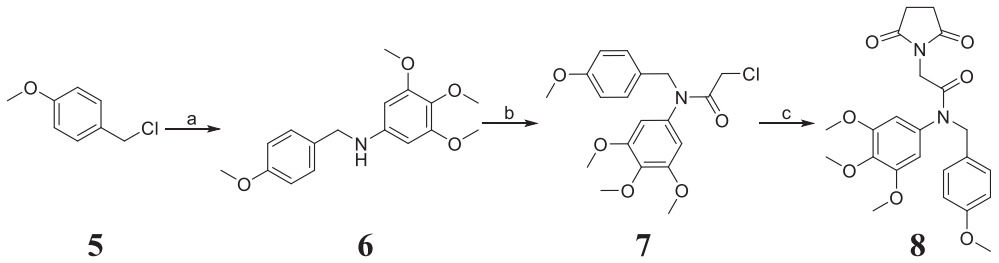

Scheme 1. Reagents and conditions. (a) Pyridine, 3,4,5-trimethoxyaniline, *N*, *N*-dimethylformamide, 60 °C. (b) Chloroacetyl chloride, K_2CO_3, acetone, room temperature. (c) Pyrrolidine-2,5-dione, KOH, acetonitrile, reflux.

was diluted to a concentration of 2 μM and applied for 48 h. The next step involved collecting cells into a 2 mL EP tube and centrifuging for 5 min at 1000 rcf and 4 °C. After resuspending cells in 70 % anhydrous alcohol, the tube was placed overnight in a –20 °C freezer for fixation. Following fixation, the tube was again centrifuged for 5 min under the same conditions, followed by discarding the supernatant. The preparation of PI staining solution was carried out following the relevant protocol. Each sample was prepared with staining buffer (0.5 mL), 20 × PI staining solution (25 μL), and 50 × RNase A (10 μL). Cells in each tube were stained with the staining solution (0.5 mL), which was mixed slowly and thoroughly and then incubated for 30 min at 37 °C in the absence of light. Finally, the role of compound **8** in the HepG2 cell cycle was examined by flow cytometry (Tian et al., 2023).

2.9. Immunofluorescence assay

After seeding onto a laser confocal dish, HepG2 cells were treated with 3 μM compound **8** for 24 h and then washed with PBS three times. The next step involved a 10-minute fixation of cells in 4 % paraformaldehyde, followed by three washes in PBS. Permeabilization was achieved using Triton X-100 (0.5 %) at room temperature for 20 min, followed by three washes in PBS. Cells were blocked for 1 h at 37 °C with 1 % BSA in PBS to reduce nonspecific background staining. Overnight incubation at 4 °C was carried out by adding 200 μL (1:400) of *β*-tubulin primary antibody solution to each dish, followed by three washes of cells in PBS for approximately 5 min each time. Next, a 1:200 dilution of DyLight 549-conjugated rabbit anti-goat secondary antibody (200 μL) was added to each dish, and a 60-minute incubation at 37 °C in the absence of light was performed. Finally, each dish was treated with 10 μg/mL DAPI staining solution (200 μL) and incubated for 10 min at room temperature in the absence of light to stain the nuclei. A laser confocal scanning microscope (Olympus FV1000, JPN) was used to observe and photograph the cells.

2.10. N, N'-ethylenebis (iodoacetamide) competition assay

After inoculation onto a 6-well microplate, HepG2 cells were incubated for 2 h with compound **8** or colchicine. Thereafter, *N*, *N*'- ethylenebis (iodoacetamide) was used to treat the cells for 1.5 h, followed by gathering of cells for western blot assessment.

2.11. Molecular docking

The 3D structure of tubulin was downloaded from the PDB repository (https://www.rcsb.org/). The PDB code of tubulin is 1SA0, and the resolution is 3.58 Å. Molecular docking between compound **8** and tubulin was performed using Autodocking tools (The Scripps Research Institute, California, United States). Molecular docking results of compound **8** were analyzed using Discovery Studio software (Beijing Tekbosi Technology Co., LTD, Beijing, China) and PyMoL software (Schrödinger, New York, United States). Various binding models, including hydrogen bonds, pi-sigma effects, carbon-hydrogen bonds, pi-donor hydrogen bonds, and van der Waals interactions, were examined in this work.

2.12. Western blotting

HepG2 cells were seeded onto a 6-well microplate, treated with the respective pharmaceuticals, and then collected with lysis buffer into 1.5-mL EP tubes. The samples were heated at 99 °C for 10 min (Hu et al., 2015). Cell lysates containing equal amounts of protein were separated by SDS-PAGE and transferred onto PVDF membranes (Merck Millipore) using electrophoresis (Bio-Red, USA). The membranes were blocked with 5 % skim milk for 1.5 h and then incubated overnight at 4 °C with primary antibodies. After three rounds of washing, the membranes were incubated with secondary antibody for 4 h at room temperature. Finally, exposure analysis was performed.

2.13. HepG2 tumor-bearing nude mice xenograft model

Male nude BALB/c mice aged 4–5 weeks were subcutaneously inoculated with DMEM (200 μL) containing 2×10^6 HepG2 cells at the right posterior dorsal area. Once their tumor volumes reached 50–100 mm^3, the mice were randomized into three groups. The experimental group received a daily intraperitoneal injection of compound **8** at 60 mg/kg, the control mice received the solvent by intraperitoneal administration once daily, and the positive group received 0.2 mg/kg of colchicine by intraperitoneal injection three times per week. The mice were regularly weighed, and their tumor volumes were estimated using the formula: tumor volume = (length × $width^2$)/2. The murine experimental protocol adhered to the guidelines for the use and care of animals approved by the Ethics Committee of Beijing University of Chinese Medicine.

2.14. Immunohistochemistry analysis

Immunohistochemical staining was conducted as per a previous procedure (Jin et al., 2017). Briefly, major organs or tumor tissues were fixed in 4 % paraformaldehyde, paraffin-embedded, stained with hematoxylin and eosin (H&E), and then subjected to immunohistochemical analysis for the indicated proteins.

2.15. Statistics

The data are presented as the mean ± SEM. Intergroup differences were assessed using the two-tailed Student's *t* test, while comparisons among multiple groups were carried out by bivariate analysis of variance with Bonferroni post hoc correction in Prism 8 (GraphPad). Statistical significance was considered at $P < 0.05$.

3. Results

3.1. Chemistry

The synthetic route of a novel pyrrolidine-2,5-dione derivative **8** is illustrated in Scheme 1. 1-(Chloromethyl)-4-methoxybenzene **5** and 3,4,5-trimethoxyaniline underwent a nucleophilic substitution reaction in the presence of pyridine to produce secondary amine **6**. In the

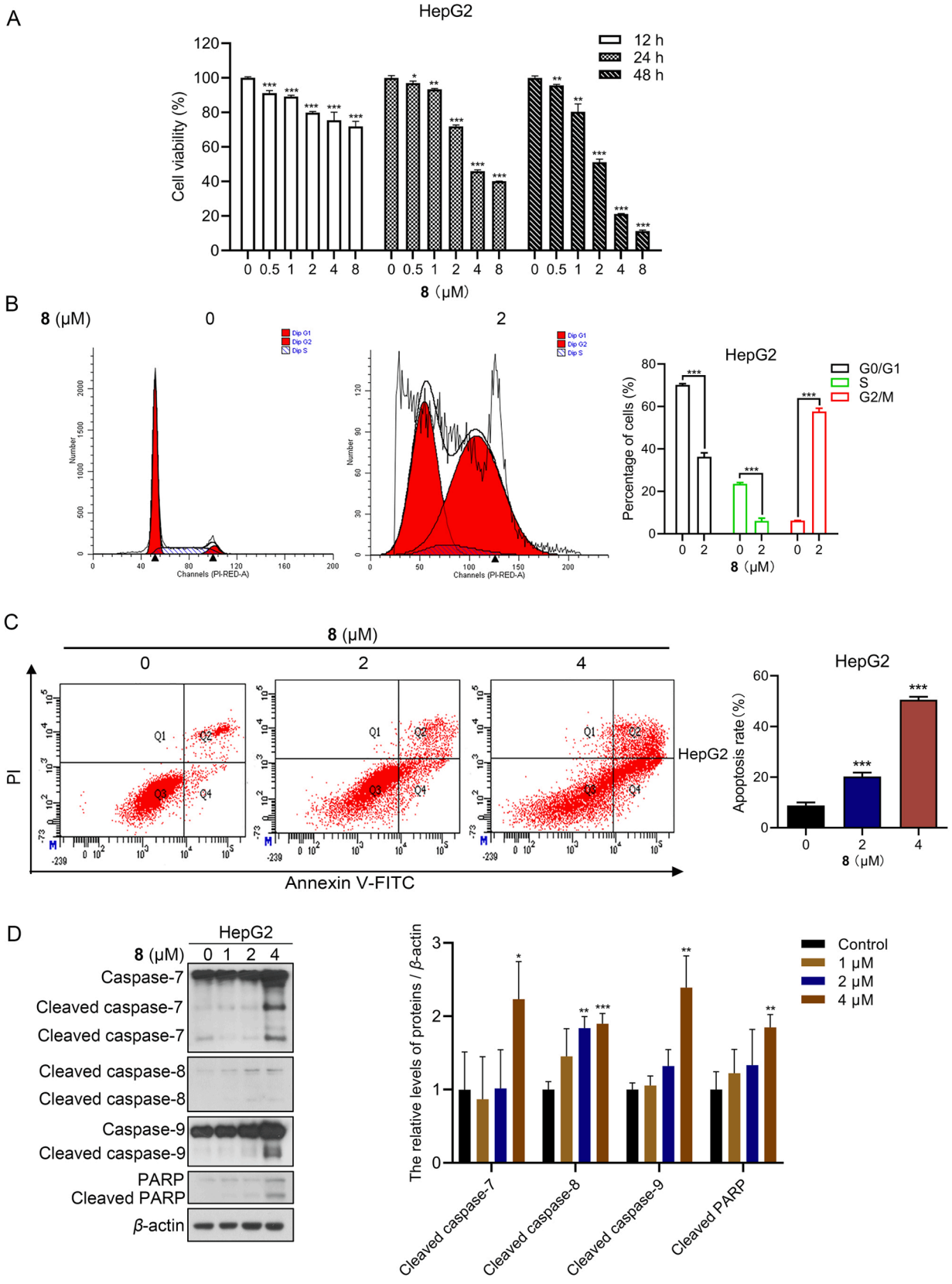

Fig. 2. Compound 8 inhibited the growth of human hepatocellular carcinoma HepG2 cells. (A) Cells were subjected to MTT viability assay after treatment with compound **8** for 12, 24, and 48 h. (B) Flow cytometric analysis of the effect of compound **8** on cell cycle distribution. (C) Flow cytometric analysis of the effect of compound **8** on apoptosis. (D) Immunoblotting analysis of apoptosis-associated protein levels in HepG2 cells treated for 24 h with or without compound **8**. $^{*}P < 0.05$, $^{**}P < 0.01$, $^{***}P < 0.001$.

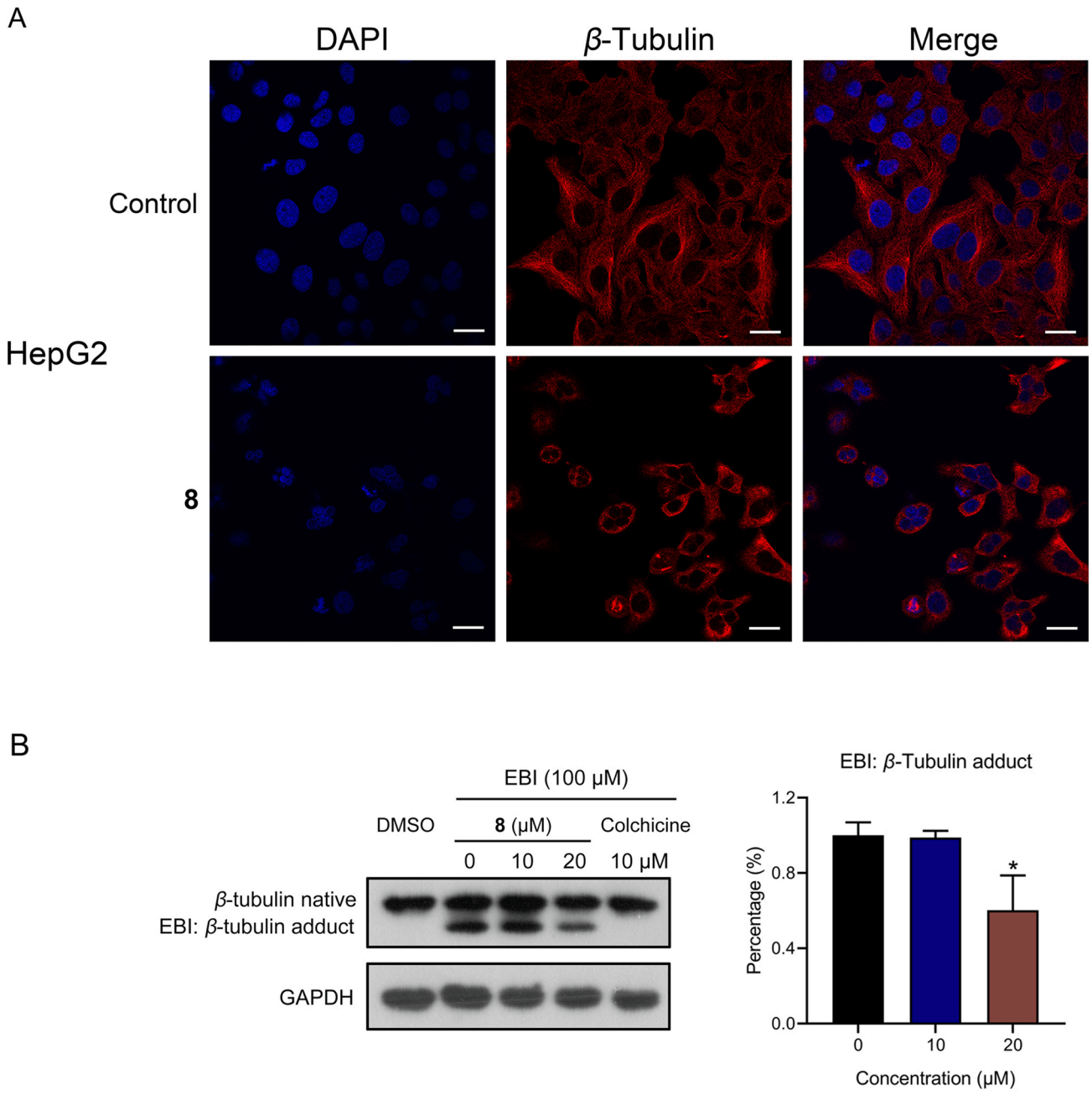

Fig. 3. Depolymerizing effect of compound 8 on the microtubule network. (A) β-tubulin staining by immunofluorescence assay. Scale bar, 20 μm. (B) EBI competition assay in HepG2 cells. *$P < 0.05$.

presence of potassium carbonate, chloroacetyl chloride reacted with secondary amine **6** via acylation to yield tertiary amide **7**. Pyrrolidine-2,5-dione was then reacted with tertiary amide **7** in the presence of potassium hydroxide to obtain target analog **8**. The chemical structures of **6** ~ **8** were characterized using NMR and MS methods, and all spectral data are provided in the Supporting Information.

3.2. Pharmacological activity

3.2.1. Compound 8 inhibited the proliferation of human hepatocellular carcinoma HepG2 cells

The anti-proliferative ability of compound **8** against human HCC HepG2 cells was assessed through the MTT assay, revealing that compound **8** significantly reduced HepG2 cell viability in a dose- and time-dependent manner. The IC_{50} value of compound **8** in HepG2 cells for 48 h was 2.082 μM (Fig. 2A).

3.2.2. Compound 8 induced G2/M phase arrest in human hepatocellular carcinoma HepG2 cells

Cell cycle dysregulation is a hallmark of proliferative disorders, and induction of cell cycle arrest is a key mechanism for inhibiting tumor cell proliferation by various classes of drugs (Mills et al., 2018, Matthews et al., 2022). Flow cytometry analysis of HepG2 cells treated with 2 μM compound **8** for 48 h showed that compound **8** induced G2/M phase arrest in human HCC cells (Fig. 2B).

3.2.3. Compound 8 induced apoptosis in human hepatocellular carcinoma HepG2 cells

Flow cytometry analysis revealed that the apoptosis rate increased gradually with the concentration of compound **8** administration, and the

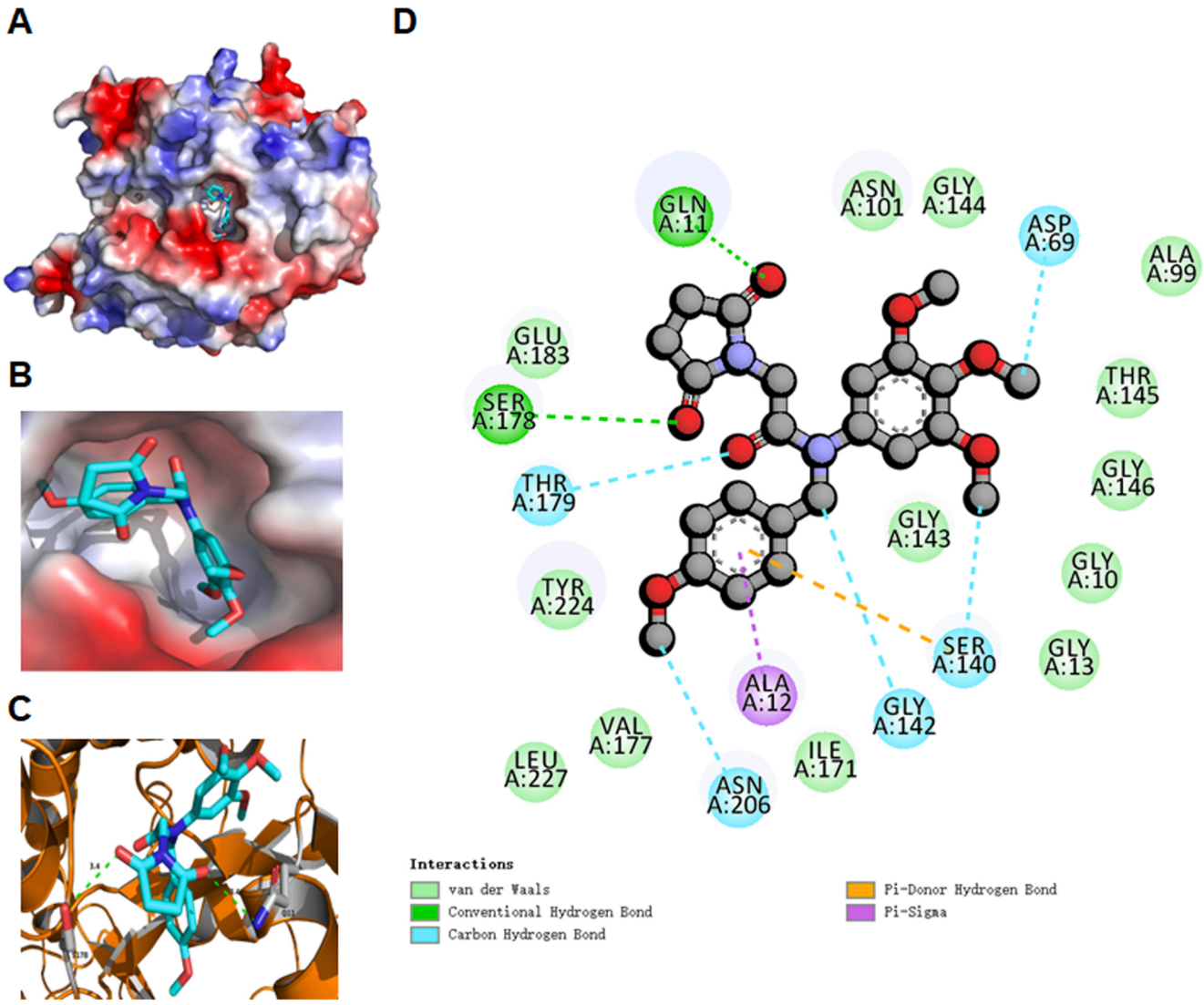

Fig. 4. Binding models of compound 8 with tubulin (PDB: 1SA0). (A) Surface map of compound **8** in tubulin. (B) Compound **8 is** located in the active pocket of tubulin. (C) Hydrogen bonds of compound **8** with surrounding residues in tubulin. (D) Detailed 2D binding models of compound **8** with residues in tubulin.

apoptosis rates of HepG2 cells treated with 2 or 4 μM compound **8** for 48 h were 20.27 %±1.55 % and 50.57 %±1.18 %, respectively (Fig. 2C). Furthermore, immunoblotting results indicated that compound **8** administration increased the protein levels of cleaved caspase−7, −8, −9, and −PARP in HepG2 cells (Fig. 2D). In summary, compound **8** was capable of inducing apoptosis in human HCC cells.

3.2.4. Compound 8 inhibited tubulin polymerization in human hepatocellular carcinoma HepG2 cells

Microtubules are built from noncovalent tubulin heterodimers (*α*- and *β*-tubulin) during a process involving polymerization and depolymerization (Perez, 2009). Owing to their crucial function in key cellular processes, particularly in mitosis, microtubules are a fascinating target for antineoplastic design (Jordan and Kamath, 2007). To investigate the effect of compound **8** on microtubules, *β*-tubulin staining was performed for immunofluorescence assessment. The results showed that unlike the representative cytoskeletal architecture of untreated cells, whose microtubules were dense and expanded throughout the cytoplasm, the cells treated with compound **8** for 24 h exhibited depolymerized microtubules. Suggestively, compound **8** inhibited the establishment of a cellular microtubule network through disruption of normal microtubule architecture in HepG2 cells, which proved that compound **8** inhibited *β*-tubulin polymerization in HepG2 cells (Fig. 3A).

The capacity of small molecules to bind to *β*-tubulin at colchicine binding sites is often evaluated via the N,N'-ethylenebis (iodoacetamide) (EBI) assay. It was discovered that the addition of compound **8** prevented EBI: *β*-tubulin adduct formation, leading to an adduct band reduction. These results indicated that compound **8** was capable of binding to *β*-tubulin's colchicine binding site directly (Fig. 3B), implying its potential as an innovative inhibitor of tubulin polymerization targeting the colchicine binding site.

3.2.5. Molecular docking studies of compound 8

Based on the potent inhibitory effects against tubulin polymerization in Fig. 3, we further investigated the binding models of compound **8** with tubulin (PDB: 1SA0). All results of the molecular docking studies are shown in Fig. 4. The surface map and 3D interaction diagram indicated that compound **8** is located in the active pocket of tubulin (Fig. 4A and 4B). Two carbonyl groups of the pyrrolidine-2,5-dione fragment in compound **8** formed two hydrogen bonds with residues SER178 and GLN11 in tubulin (Fig. 4C). The 4-methoxy phenyl ring of compound **8** formed a pi-sigma effect with ALA12 and formed a pi-donor hydrogen bond with SER140. compound **8** formed carbon hydrogen bonds with residues THR179, ASN206, GLY142, SER140 and ASP69. It also

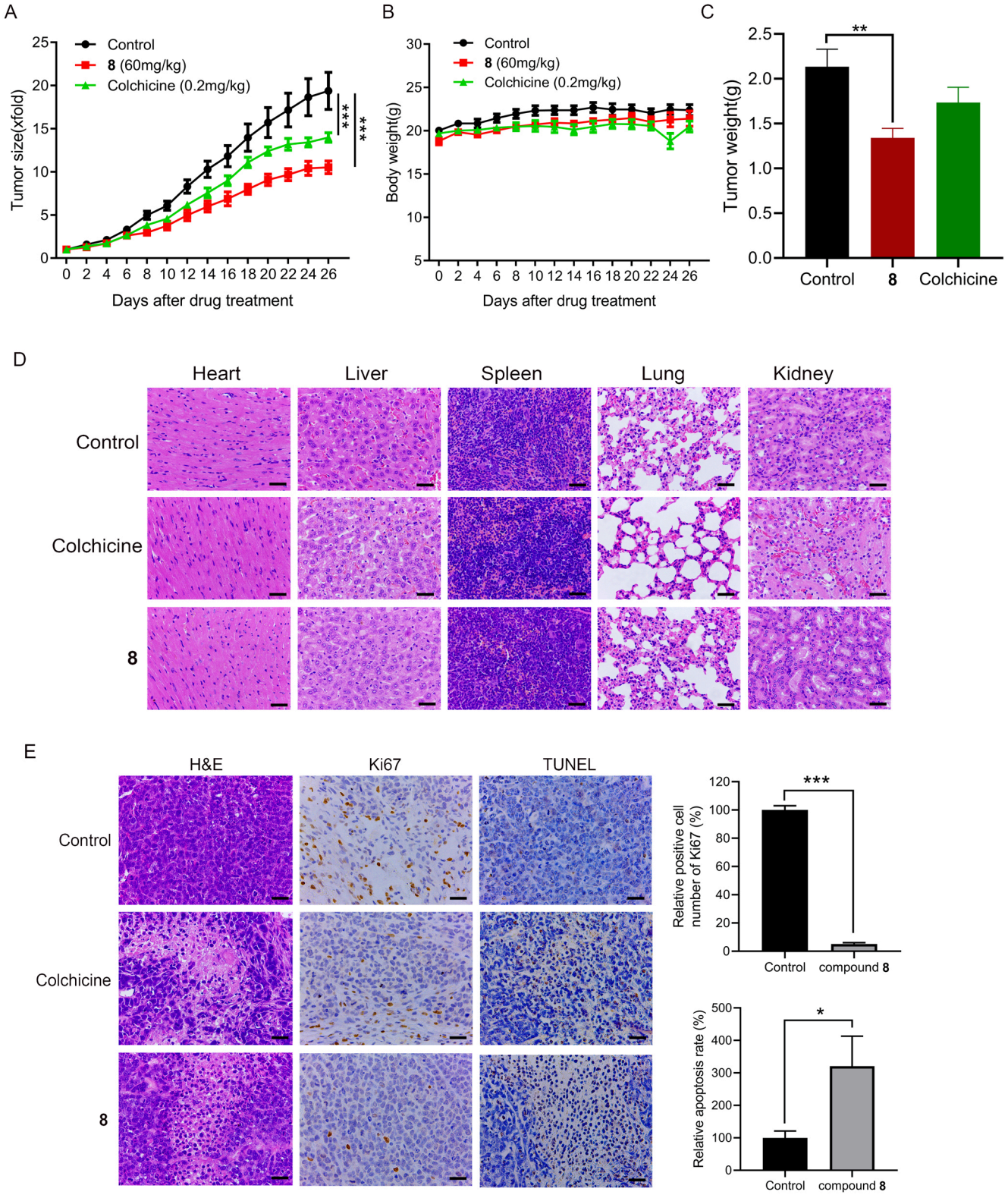

Fig. 5. Compound 8 significantly suppressed tumor growth with low toxicity in HepG2 tumor-bearing nude mice. (A) The effect of compound **8** on tumor growth in nude HepG2 tumor-bearing mice. (B) The effect of compound **8** on the murine body mass. (C) The effect of compound **8** on murine tumor weight. (D) H&E staining was performed to examine how compound **8** influenced the murine heart, lungs, liver, kidneys and spleen. (E) Tumor tissues (treated with or without compound **8**) from nude HepG2 tumor-bearing mice were subjected to TUNEL and immunohistochemical staining. Scale bars = 50 μm. $^{*}P < 0.05$, $^{**}P < 0.01$, $^{***}P < 0.001$.

generated van der Waals interactions with residues GLU183, TYR224, VAL177, LEU227, ILE171, GLY143, ASN101, GLY144, ALA99, THR145, GLY146, GLY10 and GLY13 in tubulin (Fig. 4D). The above results of molecular docking studies between compound **8** and tubulin could provide a basis for structural optimization to discover more potent tubulin polymerization inhibitors.

3.2.6. *Anti-hepatoma efficacy of compound 8 in vivo*

To investigate the antitumor impact of compound **8** *in vivo*, we utilized human hepatocellular carcinoma HepG2 cells to establish a xenograft tumor model in nude mice. As depicted in Fig. 5A and 5C, the administration of 60 mg/kg of compound **8** markedly inhibited tumor growth in the nude mice. Upon completion of the treatment, administration of compound **8** led to an approximately 45.73 % reduction in tumor volume in the mice compared to the control group. There was no significant change in the body mass of the mice after compound **8** administration (Fig. 5B). The assessment of tissue cell necrosis was performed through H&E staining (Azevedo Tosta et al., 2019). As suggested by the results of H&E staining of the heart, lungs, liver, kidneys and spleen, compound **8** displayed no marked toxicity (Fig. 5D).

3.2.7. *Effects of compound 8 on necrosis, proliferation, and apoptosis in tumor tissues of nude mice*

Compared with the control group, the tumor tissues of the compound **8**-administered group of nude mice showed more obvious necrosis, and cell membrane rupture and cell crumpling were observed in many cells from the section staining results (Fig. 5E). Ki67 is a marker closely related to proliferation. Immunohistochemical analysis showed a decreased number of cells positively stained for Ki67 in the compound **8** treatment group compared to the control group, suggesting that compound **8** inhibited cell proliferation in the tumor tissues. TUNEL staining results indicated that compound **8** treatment promoted apoptosis in the tumor tissues of nude HepG2 tumor-bearing mice (Fig. 5E).

4. Discussion

Apart from being a primary cause of fatality, cancer is also a critical obstacle to prolonging life expectancy in every global nation. Hepatocellular carcinoma is one of the most common cancers worldwide and has become a main global healthcare challenge (Vogel et al., 2022). It is imperative to accelerate the development of anti-liver cancer drugs in the clinic. For the past few years, due to desirable anticancer effects, pyrrolidine-2,5-dione has become a potential scaffold to develop anticancer agents in medicinal chemistry (Tilekar et al., 2020). In this research, we synthesized a novel pyrrolidine-2,5-dione derivative (compound **8**), which was found to have promising anti-hepatocellular carcinoma activity. Therefore, we investigated the anti-hepatocellular carcinoma effects of compound **8** and explored its potential mechanism.

Microtubules are built from noncovalent tubulin heterodimers (α- and β-tubulin) during a process involving polymerization and depolymerization (Perez, 2009). Owing to their crucial function in key cellular processes, particularly in mitosis, microtubules are a fascinating target for antineoplastic design (Jordan and Kamath, 2007). The past 10 years have seen discovery of plentiful tubulin polymerization inhibitors as powerful anticancer agents (Ghawanmeh et al., 2018). Currently, inhibitors such as AVE8062, BNC-105p, CA-4P and CKD-516 have been under clinical anti-carcinoma trials (Li et al., 2018). Plenty of microtubule inhibitors have been successfully applied to infer microtubule functionality, which is accomplished by binding to tubulin subunits (Wang et al., 2021, Muhlethaler et al., 2022, Deng et al., 2023). Multiple studies have demonstrated the pivotal role of microtubules in the regulation of mitotic spindles. Disruption of their function can often result in the obstruction of cell mitosis and its arrest, subsequently inducing apoptosis (Field et al., 2014, Barreca et al., 2020). The compound millepachine and its derivatives suppressed tubulin polymerization and invoked G2/M phase arrest of cells (Yang et al., 2018). The novel nature microtubule inhibitor ivalin invoked G2/M arrest in cell cycle and, subsequently, induced apoptosis in human HCC SMMC-7721 cells. Moreover, implication of microtubules in apoptosis mediated by Ivalin was noted (Liu et al., 2019). As a microtubule depolymerizer, tivantinib impacted the microtubule dynamics via a mechanism, invoked a G2/M phase arrest and facilitated apoptosis through both extrinsic and intrinsic pathways. It displayed a preference for resisting carcinoma growth with pro-apoptotic and anti-proliferative effects (Xiang et al., 2015). A novel resveratrol analog, by binding to its cellular target tubulin, inhibited tubulin polymerization and disturbed microtubule dynamics during the mitotic process. This led to G2/M phase arrest in the cell cycle and ultimately resulted in cell death via the intrinsic pathway of apoptosis (Thomas et al., 2016). In this study, compound **8** was a newly synthesized compound, and its impact on microtubule dynamics remains unknown. We demonstrated that compound **8** located into the active pocket of tubulin by molecular docking experiments, which prompted that compound **8** may be a novel anti-microtubule agent. To sum up, compound **8** exerted anti-HCC effect through inducing cell cycle arrest at G2/M phase and increasing apoptosis of HCC cells, which was mediated by directly targeting β-tubulin's colchicine binding site to suppress tubulin polymerization.

5. Conclusion

In brief, a novel pyrrolidine-2,5-dione derivative **8** was designed, synthesized, and evaluated for anti-hepatocellular carcinoma effects. Compound **8** significantly suppressed the HepG2 cell multiplication according to the MTT assay, and triggered G2/M phase arrest and apoptosis in HepG2 cells via flow cytometry. Moreover, compound **8** suppressed tubulin polymerization through directly binding to β-tubulin's colchicine binding site. Additionally, compound **8** was potently efficacious in fighting hepatoma *in vivo*. Therefore, compound **8** represents a promising pharmaceutical candidate for the management of HCC.

Consent for publication

Consent for publication was obtained from the participants.

Ethics statement

The animal experiment was also approved by the Ethics Committee of Beijing University of Chinese Medicine. Great efforts were made to minimize the number of animals used in the experiments and their discomfort.

CRediT authorship contribution statement

Yingying Tian: Investigation, Methodology, Data curation, Visualization, Writing – original draft. **Ailin Yang:** Investigation, Formal analysis, Validation. **Huiming Huang:** Investigation, Formal analysis, Validation. **Jinxin Xie:** Investigation, Formal analysis, Validation. **Longyan Wang:** Investigation, Formal analysis, Validation. **Dongxiao Liu:** Investigation, Formal analysis, Validation. **Xuejiao Wei:** Investigation, Formal analysis, Validation. **Peng Tan:** Investigation, Formal analysis, Validation. **Pengfei Tu:** Formal analysis, Methodology. **Dongjun Fu:** Conceptualization, Supervision, Funding acquisition, Writing – review & editing. **Zhongdong Hu:** Conceptualization, Supervision, Funding acquisition, Writing – review & editing.

Declaration of competing interest

The authors declare that they have no known competing financial interests or personal relationships that could have appeared to influence the work reported in this paper.

Acknowledgements

This study was financially supported by the National Natural Science Foundation of China, China; (82074072, 81873044), the Beijing Nova Program of Science and Technology, China (Z191100001119083), the Fundamental Research Funds for the Central Universities, China (2023-JYB-JBQN-051, 2022-JYB-XJSJJ025), and the Talent Cultivation Project of Beijing University of Chinese Medicine, China (JZPY202206).

Appendix A. Supplementary material

Supplementary data to this article can be found online at https://doi.org/10.1016/j.arabjc.2023.105550.

References

Azevedo Tosta, T.A., de Faria, P.R., Neves, L.A., et al., 2019. Computational normalization of H&E-stained histological images: progress, challenges and future potential. Artif. Intell. Med. 95, 118–132. https://doi.org/10.1016/j.artmed.2018.10.004.

Barreca, M., Stathis, A., Barraja, P., et al., 2020. An overview on anti-tubulin agents for the treatment of lymphoma patients. Pharmacol. Ther. 211, 107552 https://doi.org/10.1016/j.pharmthera.2020.107552.

Chen, X., Zhao, Y., Yang, A., et al., 2020. Chinese dragon's blood EtOAc extract inhibits liver cancer growth through downregulation of Smad3. Front. Pharmacol. 11, 669. https://doi.org/10.3389/fphar.2020.00669.

Deng, S., Banerjee, S., Chen, H., et al., 2023. SB226, an inhibitor of tubulin polymerization, inhibits paclitaxel-resistant melanoma growth and spontaneous metastasis. Cancer Lett. 555, 216046 https://doi.org/10.1016/j.canlet.2022.216046.

Field, J.J., Kanakkanthara, A., Miller, J.H., 2014. Microtubule-targeting agents are clinically successful due to both mitotic and interphase impairment of microtubule function. Bioorg. Med. Chem. 22, 5050–5059. https://doi.org/10.1016/j.bmc.2014.02.035.

Fu, D.J., Yang, J.J., Li, P., et al., 2018. Bioactive heterocycles containing a 3,4,5-trimethoxyphenyl fragment exerting potent antiproliferative activity through microtubule destabilization. Eur. J. Med. Chem. 157, 50–61. https://doi.org/10.1016/j.ejmech.2018.07.060.

Ghawanmeh, A.A., Chong, K.F., Sarkar, S.M., et al., 2018. Colchicine prodrugs and codrugs: Chemistry and bioactivities. Eur. J. Med. Chem. 144, 229–242. https://doi.org/10.1016/j.ejmech.2017.12.029.

Goodson, H.V., Jonasson, E.M., 2018. Microtubules and microtubule-associated proteins. Cold Spring Harb. Perspect. Biol. 10 https://doi.org/10.1101/cshperspect.a022608.

Guggilapu, S.D., Guntuku, L., Reddy, T.S., et al., 2017. Synthesis of thiazole linked indolyl-3-glyoxylamide derivatives as tubulin polymerization inhibitors. Eur. J. Med. Chem. 138, 83–95. https://doi.org/10.1016/j.ejmech.2017.06.025.

Han, S.H., Kim, S., De, U., et al., 2016. Synthesis of succinimide-containing chromones, naphthoquinones, and xanthones under Rh(III) catalysis: evaluation of anticancer activity. J. Org. Chem. 81, 12416–12425. https://doi.org/10.1021/acs.joc.6b02577.

Ho, S.T., Lin, C.C., Tung, Y.T., et al., 2019. Molecular mechanisms underlying Yatein-induced cell-cycle arrest and microtubule destabilization in human lung adenocarcinoma cells. Cancers (Basel) 11. https://doi.org/10.3390/cancers11091384.

Hu, Z., Wang, Y., Huang, F., et al., 2015. Brain-expressed X-linked 2 is pivotal for hyperactive mechanistic target of rapamycin (mTOR)-mediated tumorigenesis. J. Biol. Chem. 290, 25756–25765. https://doi.org/10.1074/jbc.M115.665208.

Jin, F., Jiang, K., Ji, S., et al., 2017. Deficient TSC1/TSC2-complex suppression of SOX9-osteopontin-AKT signalling cascade constrains tumour growth in tuberous sclerosis complex. Hum. Mol. Genet. 26, 407–419. https://doi.org/10.1093/hmg/ddw397.

Jordan, M.A., Kamath, K., 2007. How do microtubule-targeted drugs work? An overview. Curr. Cancer Drug Targets. 7, 730–742. https://doi.org/10.2174/156800907783220417.

Li, L., Jiang, S., Li, X., et al., 2018. Recent advances in trimethoxyphenyl (TMP) based tubulin inhibitors targeting the colchicine binding site. Eur. J. Med. Chem. 151, 482–494. https://doi.org/10.1016/j.ejmech.2018.04.011.

Liu, F., Lin, S., Zhang, C., et al., 2019. The novel nature microtubule inhibitor ivalin induces G2/M arrest and apoptosis in human hepatocellular carcinoma SMMC-7721 cells in vitro. Medicina (Kaunas) 55. https://doi.org/10.3390/medicina55080470.

Luzina, E.L., Popov, A.V., 2014. Synthesis and anticancer activity evaluation of 3,4-mono- and bicyclosubstituted N-(het)aryl trifluoromethyl succinimides. J. Fluor. Chem. 168, 121–127. https://doi.org/10.1016/j.jfluchem.2014.09.019.

Matthews, H.K., Bertoli, C., de Bruin, R.A.M., 2022. Cell cycle control in cancer. Nat. Rev. Mol. Cell Biol. 23, 74–88. https://doi.org/10.1038/s41580-021-00404-3.

Mills, C.C., Kolb, E.A., Sampson, V.B., 2018. Development of chemotherapy with cell-cycle inhibitors for adult and pediatric cancer therapy. Cancer Res. 78, 320–325. https://doi.org/10.1158/0008-5472.CAN-17-2782.

Milosevic, N.P., Kojic, V., Curcic, J., et al., 2017. Evaluation of in silico pharmacokinetic properties and in vitro cytotoxic activity of selected newly synthesized N-succinimide derivatives. J. Pharm. Biomed. Anal. 137, 252–257. https://doi.org/10.1016/j.jpba.2017.01.042.

Muhlethaler, T., Milanos, L., Ortega, J.A., et al., 2022. Rational design of a novel tubulin inhibitor with a unique mechanism of action. Angew. Chem. Int. Ed. Engl. 61, e202204052.

Ouyang, L., Li, J., Chen, X., et al., 2023. Chinese dragon's blood ethyl acetate extract suppresses gastric cancer progression through induction of apoptosis and autophagy mediated by activation of MAPK and downregulation of the mTOR-Beclin1 signalling cascade. Phytother. Res. 37, 689–701. https://doi.org/10.1002/ptr.7652.

Perez, E.A., 2009. Microtubule inhibitors: Differentiating tubulin-inhibiting agents based on mechanisms of action, clinical activity, and resistance. Mol. Cancer Ther. 8, 2086–2095. https://doi.org/10.1158/1535-7163.MCT-09-0366.

Sun, V.C., Sarna, L., 2008. Symptom management in hepatocellular carcinoma. Clin. J. Oncol. Nurs. 12, 759–766. https://doi.org/10.1188/08.CJON.759-766.

Sung, H., Ferlay, J., Siegel, R.L., et al., 2021. Global Cancer Statistics 2020: GLOBOCAN Estimates of Incidence and Mortality Worldwide for 36 Cancers in 185 Countries. CA Cancer J. Clin. 71, 209–249. https://doi.org/10.3322/caac.21660.

Thomas, E., Gopalakrishnan, V., Hegde, M., et al., 2016. A novel resveratrol based tubulin inhibitor induces mitotic arrest and activates apoptosis in cancer cells. Sci. Rep. 6, 34653. https://doi.org/10.1038/srep34653.

Tian, Y., Wang, L., Chen, X., et al., 2023. DHMMF, a natural flavonoid from Resina Draconis, inhibits hepatocellular carcinoma progression via inducing apoptosis and G2/M phase arrest mediated by DNA damage-driven upregulation of p21. Biochem. Pharmacol. 211, 115518 https://doi.org/10.1016/j.bcp.2023.115518.

Tilekar, K., Upadhyay, N., Meyer-Almes, F.J., et al., 2020. Synthesis and biological evaluation of Pyrazoline and Pyrrolidine-2,5-dione hybrids as potential antitumor agents. ChemMedChem 15, 1813–1825. https://doi.org/10.1002/cmdc.202000458.

Vogel, A., Meyer, T., Sapisochin, G., et al., 2022. Hepatocellular carcinoma. Lancet 400, 1345–1362. https://doi.org/10.1016/S0140-6736(22)01200-4.

Wang, P., Xiao, X., Zhang, Y., et al., 2021. A dual inhibitor overcomes drug-resistant FLT3-ITD acute myeloid leukemia. J. Hematol. Oncol. 14, 105. https://doi.org/10.1186/s13045-021-01098-y.

Xiang, Q., Zhen, Z., Deng, D.Y., et al., 2015. Tivantinib induces G2/M arrest and apoptosis by disrupting tubulin polymerization in hepatocellular carcinoma. J. Exp. Clin. Cancer Res. 34, 118. https://doi.org/10.1186/s13046-015-0238-2.

Yang, J., Yan, W., Yu, Y., et al., 2018. The compound millepachine and its derivatives inhibit tubulin polymerization by irreversibly binding to the colchicine-binding site in beta-tubulin. J. Biol. Chem. 293, 9461–9472. https://doi.org/10.1074/jbc.RA117.001658.